CHAPTETER V

SYNTHESIS OF Ti-MCM-41 DIRECTLY FROM SILATRANE AND TITANIUM GLYCOLATE AND ITS ACTIVITY

5.1 Abstract

Titanium is successfully incorporated in hexagonal mesoporous silica to form Ti-MCM41 at low temperature. Silatrane and titanium glycolate synthesized from the Oxide One Pot Synthesis (OOPS) process are used as the precursors. Using cationic surfactant, cetyltrimethylammonium bromide, as a template, the resulting meso-structure mimics the liquid crystal phase. The percentage of Ti loading is varied in the range of 1-35%. The temperatures used to prepare are 60° and 80°C. After heat treatment, very high surface area mesoporous silica was obtained and characterized using DRUV, XRD, BET, XRF, EDS and TEM. At 35% Ti, Ti atom is also in the frame work showing the pattern of hexagonal mesostructure, as shown by DRUV, XRD and TEM results. The surface area is extraordinarily high, up to more than 2300 m^2/g while the pore volume is as high as 1.3 cc/g for Ti loading range of 1-5%. Oxidative bromination reaction using Ti-MCM-41 as catalyst showed impressive result, with the 60°C catalysts having higher activity.

5.2 Introduction

Catalytic oxidation is an important process in production of fine chemicals. It was discovered that TS-1 and its extension as TS-β and TS-ZSM are active for selective oxidation of various compounds in the presence of hydrogen peroxide [1]. However, large organic molecule cannot access the active sites located inside the small cavities and channels of the zeolite. Larger pore zeolites, M41S family was discovered by Mobil researchers. The new materials designated as mesoporous molecular sieves (MMSs) include hexagonal MCM-41, cubic MCM-48 and lamellar MCM-50 phases [2]. The preparation of M41S family involves liquid crystal

formation by the cationic surfactant, cetyltrimethylammonium bromide (CTAB) [3-5]. The high surface area (over 1000 m^2g^{-1}) , monodisperse pore sizes in the range of 2-50 nm, and a high degree of stereoregularity mimicking the liquid crystal structure used in their preparation, results in a catalyst with almost no mass transfer limitation. In addition, titanium supported on MMS showed a promising oxidation reaction of large organic molecules with hydrogen peroxide as the oxidizing agent and it could also be used as a photocatalyst.

Ti –Incorporated MCM 41 was prepared by either grafting titanium precursor on to surface silanols via post-synthetic procedure or depositing titanium precursor on MCM-41 from the sol obtained by controlled hydrolysis of titanium alkoxide precursor followed by calcination. In this paper, metal alkoxide precursors, viz. silatrane and titanium glycolate, were used for producing mesostructure materials due to their moisture stability, resulting in the ability to control hydrolysis and condensation. The precursors were synthesized directly from inexpensive metal oxide SiO_2 and TiO_2 via the "Oxide One Pot Synthesis (OOPS)" process. This process gave high purity of metal alkoxide products, having been successfully used for syntheses of high quality microporous zeolites, such as LTA [6], ANA and GIS [7] and MFI [8]. In general, the most active and selective sites of titanium-supported heterogeneous catalyst are isolated, mononuclear, 4-coordinated Ti(IV) centers.

It has been recognized that the most promising oxidation catalyst is the catalyst containing isolated active sites, meaning one or only a few metal incorporated centers on the surface of an oxide support. Typically, these active sites are associated with a specific inorganic structure, giving rise to the desired catalytic properties. Thus, the highlight of this paper is to prepare high percent loading of Ti incorporated MCM 41 with high surface area while maintaining MCM-41 hexagonal structure, to provide the highest concentration of active sites per unit volume of catalyst.

5.3 Experimental

5.3.1 Materials

Fumed silica (SiO_2) was purchased from Aldrich Chemical Co. Titanium dioxide, potassium bromide (KBr) and hydrogen peroxide (H_2O_2) were purchased from Carlo Erba. 2-[(4-hydroxyphenyl)(4-oxo-2,5-cyclohexadien-1-ylidene)methyl]benzene sulfonic acid (phenol red), ethylene glycol ($HOCH_2CH_2OH$) and triethanolamine (TEA, $N(CH_2CH_2OH)_3$) were supplied by Labscan Asia Co., and used as received. Acetronitrile (CH_3CN) was also obtained from Labscan Asia Co. and distilled before use. Cetyltrimethylammonium bromide (CTAB) and sodium hydroxide were purchased from Sigma Chemical Co. HEPES buffer solution (4-(2-hydroxyethyl)-1-piperazineethanesulfonic acid) was obtained from Fluka.

5.3.2 Materials Characterization

Mass spectra of precursors were obtained on a FISONS Instruments 707 VG Autospec-ultima mass spectrometer (Manchester, England) with VG data system, using the positive fast atom bombardment (FAB^+-MS) mode. FTIR spectroscopic analysis was conducted using a Bruker Instrument (EQUINOX55) with a resolution of 4 cm^{-1}. The solid sample was prepared by mixing 1% of sample with anhydrous KBr. Thermal properties were analyzed using Du Pont Instrument TGA 2950 thermogravimetric analysis (TGA).

The mesoporous product was characterized using a Rigaku X-ray diffractometer (XRD) with CuKα source at a scanning speed of 0.75 degree/sec. The working range was 2θ = 1.5-10. Electron microscope study (TEM micrographs and electron diffraction patterns) were carried out using JEOL 2010F. Surface area and average pore size were determined by BET method using a Quantasorb JR. (Autosorb-1). The product was degassed at 250°C for 12 hr prior to analysis. Diffuse reflectance ultraviolet spectroscopy was used to identify the location and the coordination of titanium in hexagonal structure. The reflectance output from the instrument was converted using Kubelka-Munk algorithm. The titanium content was characterized using SEM/EDS and XRF. The calcination was conducted using a Carbolite Furnace (CFS 1200) with the heating rate of 1°C/min.

5.3.3 Silatrane Synthesis

Wongkasemjit's [9-10] synthetic method was followed by mixing silicon dioxide (0.10 mol, 6 g), and triethanolamine (0.125 mol, 18.6 g) in a simple distillation set using 100 mL ethylene glycol solvent. The reaction was done at the boiling point of ethylene glycol under nitrogen atmosphere to remove water as a by-product along with ethylene glycol from the system. The reaction was run for 10 hr and excess ethylene glycol was removed under vacuum (1.6 Pa) at 110°C. The brownish white solid was washed with dried acetonitrile for three times. The white powder product was characterized using FTIR, TGA and FAB^+-MS.

FTIR bands observed were: 3000-3700 cm^{-1} (w, intermolecular hydrogen bonding of O-H), 2860-2986 cm^{-1} (s, νC-H), 1244-1275 cm^{-1} (m, νC-N), 1170-1117 (bs, νSi-O), 1093 (s, νSi-O-C), 1073 (s, νC-O), 1049 (s, νSi-O), 1021 (s, νC-O), 785 and 729 (s, νSi-O-C) and 579 cm^{-1} (w, Si<---N). TGA showed one sharp mass loss transition at 390°C and gave 18.5% ceramic yield corresponding to $Si((OCH_2CH_2)_3N)_2H_2$. FAB^+-MS showed the highest m/e at 669 of $Si_3((OCH_2CH_2)_3N)_4H^+$ and 100% intensity at 323 of $Si((OCH_2CH_2)_3N)_2H^+$.

5.3.4 Titanium Glycolate Synthesis

A mixture of titanium dioxide (0.025 mol, 2 g), triethylenetetramine (0.007 mol, 3.7 g), used as a catalyst, and 25 mL of ethylene glycol, used as a solvent, were heated to the boiling point of EG for 24 hr, followed by separating the unreacted TiO_2 from the solution part. The excess EG and TETA were removed by vacuum distillation to obtain the crude white solid product. The crude product was then washed with acetonitrile and dried in a vacuum desiccator before characterization using FTIR, TGA, and FAB^+-MS [11].

FTIR bands observed were: 3000-3700 cm^{-1} (w, trace of water absorbed in the product), 2860-2986 cm^{-1} (s, νC-H), 1244-1275 cm^{-1} (m, νC-N), 1170-1117 (bs, νSi-O), 1093 (s, νSi-O-C), 1073 (s, νC-O), 1049 (s, νSi-O), 1021 (s, νC-O), 785 and 729 (s, νSi-O-C) and 579 cm^{-1} (w, Si<---N). TGA result showed one sharp mass

loss corresponding to the decomposition of organic ligand and remaining organic residue around 310°-350°C and gave 46.8% ceramic yield which is close to the theoretical yield of 47.5%. FAB^+-MS: showed m/e 169 with 8.5% intensity of $Ti(OCH_2CH_2O)_2$.

5.3.5 Synthesis of Ti-MCM-41

Various ratios of silatrane and titanium glycolate precursors in the range of 1-35 % Ti were studied by adding into a solution containing 112 x 10^{-5} mol CTAB, 1 x 10^{-3} mol NaOH and 14 x 10^{-3} mol TEA. 36 x 10^{-2} mol of water was then added with vigorous stirring at 60° and 80°C. The mixture was stirred for various times to follow the reaction using DRUV. The obtained crude product was filtered and washed with water to obtain a white solid. The white solid was dried at room temperature and calcined at 550°C for 3 hr to obtain mesoporous Ti-MCM-41 characterized using XRD, XRF, EDS, BET and TEM.

5.3.6 Catalytic Activity Study

The peroxidative bromination test was used to qualitatively study catalyst activity. Ti-MCM-41 was added into a mixture of 0.2 mM phenol red, 0.1 M.KBr, 10 mM H_2O_2 in 0.1M HEPES buffer having pH 6.5. Then, the mixture was stirred for various times. The total volume of the mixture was 3.5 mL. The formation of 2-[(3,5-dibromo-4-hydroxyphenyl)(3,5-dibromo-4-oxo-2,5-cyclohexadienylidene)methyl benzenesulfonic acid (bromophenol blue) from phenol red was monitored by UV-vis after removing the solid catalyst.

5.4 Results and Discussion

5.4.1 Ti-MCM41 Characterization

DRUV was used to determine the site of titanium and to determine the presence of extra-framework Ti in our synthesized Ti-MCM41. In general, DRUV absorbance pattern depends on Ti content, synthesis procedure used and site where Ti is incorporated [12-15]. For small amounts of well dispersed Ti, DRUV peak will show only an isolated, tetrahedrally coordinated species, as indicated by the peak at λ= 200-230 nm, see fig.5.1 when the incorporated Ti is not more than 5%. The band can be interpreted as a ligand metal charge transfer transition from oxygen to isolated tetrahedral Ti(IV) [16-17]. In case of more than 4 coordination number, such as bonding with water molecules beside the metal coordination sphere, the absorption band will be shifted to the longer wavelengths or lower energies. In fig.5.1, 1-10%Ti incorporated MCM-41 are almost in the form of isolated Ti(IV), referring to the presence of the intense band mainly around 220 nm, for both 60°and 80°C reaction temperatures. However, as increasing the Ti content, the DRUV band is a little bit shifted to longer wavenumbers, probably due to ligand to metal charge transfer involving isolated Ti atoms in octahedral environment, from which two water molecules are bonded [13-14]. In fact, it has been reported that materials containing small amount of well dispersed Ti ($\approx$ 2%) will generally form isolated tetrahedrally coordinated Ti [16], as reported by Maschmeyer and coworkers that TEA was found to act not only as a template but also a director for positioning Ti-site to form isolated tetrahedrally coordinated Ti species [18]. When %Ti increased, the DRUV peak was broader and showed very small shoulder at λ= 280 nm, as shown in fig.5.2. This peak pattern corresponds to partially polymerized Ti species (five- and six coordinated) [15, 19]. The red shift and broad band for Ti-mesoporous samples may be an indication that at higher Ti contents, there is a higher possibility of Ti to form either disordered tetrahedral environment or octahedral coordination spheres. From the fact that DRUV is a sensitive instrument for detecting the extra-framework of Ti absorption around 330 nm, the band spectra at 330 nm did not appear in our samples, meaning that the extra-framework or cluster of Ti in MCM-41 was not present for all studied conditions. This implies that our synthesized silatrane and titanium glycolate hydrolyze and condense together very well. Amoros *et al* also synthesized mesoporous oxide using silatrane and titanatrane precursors [3-5, 20-22] to form

high %Ti containing mesoporous silica for epoxidation study. In their work, the minimum Si/Ti ratio was as low as 1.9 [20]. Their success came from the ability to control hydrolysis and condensation processes. Silatrane is quite inert towards hydrolysis comparing with other alkoxide precursors, thus it facilitates the users to introduce highly active tetrahedral site Ti into mesoporous silica. However, titanatrane was not as inert for hydrolysis as reported by Amoros *et al.* Titanium glycolate in our work, on the other hand, is much more stable, thus, the synthesis provided higher %Ti incorporated into MCM-41. Comparing synthesis at 60° and 80°C, the higher temperature gave a broader band and showed a more intense shoulder at λ=280 nm (Fig.5.3), indicating the presence of higher concentration of partially polymerized Ti species (contain more Ti-O-Ti bonds) [19]. This result was probably due to the sensitivity of both silatrane and titanium glycolate precursors towards higher temperature.

The calcined products at various %Ti contents showed a well-resolved pattern of hexagonal mesostructure, as shown in fig.5.4. In this figure, XRD spectra give only hk0 reflections and no reflections at diffraction angles larger than 6 degree 2θ were observed. The positions of these peaks approximately fit with the position for the hk0 reflections of a hexagonal unit cell with a = b and c = ∞ [23-24]. The three-peak positions of 100, 110 and 200 reflections are from long range structural order of hexagonal arrays. However, at high %Ti, the XRD patterns showed the lower crystalline material, as indicated by the lower intensity of 100 reflections peak, the smaller and less isolate of 110 and 200 reflections peaks. Nevertheless, when %Ti is more than 10, the 3 hr synthesis time is not enough for hexagonal array to form, as can be seen in the XRD spectrum containing no 110 and 200 reflections. This is in agreement with those reported in references 25-27. However, after increasing the synthesis time to 8 hr, the 110 and 200 reflections appeared again due to larger size of Ti ions needing more time to diffuse into the lattice sites [29]. Thus, at high Ti content longer times are needed for diffusion and condensation into the hexagonal pattern. Increasing Ti loading up to 35% resulted in the disappearance of 110 and 200 reflections, as shown in fig.5.5. However, the pattern of MCM-41 was still remained. It is the highlight of our work that the pattern of MCM-41 can be

retained as high %Ti loading was incorporated. The main reason for this result probably comes from our extraordinary alkoxide precursors, silatrane and titanium glycolate, having highly pure and moisture stable properties. Ozin *et al* also used glycometallate precursor to prepare hexagonal mesoporous silica. The non-aqueous lamella phase of glycometallate precursor changed into hexagonal meso-phase when hydrolyzed with water [30-31]. However, it needed post-treatment with Si_2H_6 to re-enforcement meso-structure due to the collapse of unstable product structure upon the removal of surfactant template. The collapsed structure referring to insufficient degree of silica polymerization may arise from the structure defect during phase transformation.

FTIR spectra of Ti-MCM-41 are shown in fig. 5.6, the absorption peak at 970 cm^{-1} is assigned to the vibrational peak of titanium silicate and considered as the fingerprint of the titanium framework. It was first assigned as Ti=O group [25] However, this peak assignment was later discounted and interpreted in terms of Si-OH groups and Ti-O-Si bonds [25-26]. The 950-970 cm^{-1} band is increased in the intensity with increasing %Ti. This result was explained by 970 cm^{-1} band being essentially due to the increased degeneracy of the elongation vibration in the tetrahedral structure of SiO_4 induced by the change in the polarity of the Ti-O bonds when Si is linked to Ti [25-26]. The SiOH groups sharing the OH group with Ti are then responsible for the absorption at higher wavenumbers compared to the unshared Si-OH group.

Nitrogen physisorption probes the textural properties of materials, such as surface area, pore size, pore volume and pore geometry. The nitrogen adsorption/desorption isotherm of pure Ti-MCM-41 at various Ti loadings are shown in fig. 5.7. The BET surface area, pore size and pore volume of Ti-MCM-41 are summarized in Table 5.1. Fig.5.7, shows that all the isotherms are of type IV classification of IUPAC with five distinct regions. At low relative pressure (P/Po) a very large amount of nitrogen becomes physisorbed in form of monolayer on the surface of MCM-41 (both inside and on the external surface of the mesopore). Region II is the multilayer adsorption. From fig 5.7, Region III shows a sharp inflection with relative pressure > 0.3, characteristics of capillary condensation within uniform pores. Because filling of the mesopores takes place over a relatively

small range of relative pressure, indicative of nearly equal sized pores. A further support for this interpretation is that the desorption curve almost completely coincides with the adsorption isotherm in this pressure range. Surprisingly, table 5.1 shows that at higher amount of Ti loading, the pore size was increased. This is opposite to many papers stating that the higher amount of Ti loading decreased the pore size. However, it was also noticed by Bharat in 2001 that an increase in the mesopore size was observed when increasing Ti loading with the microwave technique. This result corresponds to a decrease in pore wall thickness of the crystallite sample and indicates that the titanium substituted MCM-41 could be crystallized without decreasing mesopore size via our normal synthesis process. The BET surface areas of our synthesized Ti-MCM-41 are very high comparing with others [25-27] whereas pore size is comparable. From our previous work, the synthesis of MCM-41 by controlling ion concentration, reaction time, reaction temperature and surfactant concentration resulted in remarkably high surface area MCM-41 significantly increased from 1100 to around 2000m^2/g [32]. Again, the main reason comes from the fact that our highly pure and moisture stable silatrane and titanium glycolate can be manipulated to achieve the balance between hydrolysis and condensation reactions for the extremely high surface area MCM-41 synthesis. Amoros *et al,* who also used silatrane as precursor [20], obtained smaller surface area probably due to the difference of precursor synthesis methods giving different silatrane derivatives, hence providing different precursor reactivity.

To confirm the XRD results, TEM image of MCM-41 at 60°C was analyzed and is shown in fig.5.8, showing in the perpendicular direction in which cylindrical cross sections of the channels are clearly visible [24]. The periodicity of the pore size calculated from the TEM image is 2.35 nm for unloaded MCM-41 and 2.2 nm for 5%Ti loaded MCM-41. The %Ti incorporation was determined using both XRF and EDS. The results showed that Ti incorporated is almost the same as experimental Ti loading, as summarized in table 5.2.

5.4.2 Catalytic Activity

Transition metal ions isomorphously substituted into the tetrahedral framework of micro and mesoporous molecular sieve are promising catalyst applications. Their activity includes hydroxylation, epoxidation and oxidation reaction. Because of their large surface area and monodispersed pore size, they offer the opportunity to create reaction sites and molecular confinement which permit the selective product to form, especially in biocatalytic process. Peroxidative bromination is successfully catalyzed using vanadium bromoperoxidase (V-BrPO) and hydrogen peroxide as an oxidant under mild condition [28]. Ti-MCM-41 has been discovered to biomimic the function of vanadium bromoperoxidase at neutral pH [29, 33-34]. Phenol red, λ_{max}= 450 nm, would be transformed into bromophenol blue, λ_{max}= 589 nm, [34] when reacted with only small amount of Ti-MCM41 catalyst (3-5mg). The structures of phenol red and bromophenol blue are illustrated in equation 1 and the formation of bromophenol blue from phenol red in this work was monitored and shown in fig.5.9.

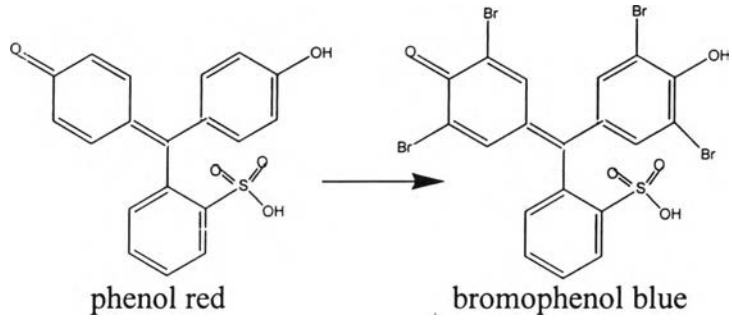

phenol red bromophenol blue (1)

As shown in fig.5.9, increasing the reaction time the absorbance at λ_{max}= 589 nm increased indicating the increasing bromination of phenol red to form bromophenol blue with time. It was reported that the function of Ti (IV) is to coordinate and activate H_2O_2 for bromine oxidation represented by an absorbance band at 400 nm. The results are consistent with the formation of peroxotitanium species [35]. Fig 5.10 shows the plots of absorbance band of 589 nm with various times and various %Ti loadings. Additionally, MCM-41 containing no Ti was also tested its activity, and it was found that the bromination reaction does not occur, as can be seen in the graph. This evidence was also reported in reference 34 when

MCM-41 and MCM-48 were studied. If the solution mixture was kept stirred for 56 hr, the absorbance at 589 nm was detected. The intensity is comparable with the intensity of 10% Ti loading detected at 90 min reaction time. The same conditions were studied in the case of TiO_2, it was indicated that no activity at the time studied was observed. However, after continuously stirred for almost 30 hr the solution gradually turned to blue. The absorbance intensity increases when increasing % Ti loading at the same reaction time. Interestingly, the activity kept increasing although 35% Ti was loaded. This result indeed indicates no cluster titania formation which is coincident with the DRUV results. If a cluster of titanium was formed, it would not be accessible for peroxide coordination, resulting in limited active catalyst.

As for the effect of the reaction temperature, 60° and 80°C, see Fig.5.11, the activity of catalyst prepared at 60°C is better since the presence of higher absorbance band at λ_{max}= 589 nm is detected at the same reaction time. The reason comes from more partially polymerized Ti species formed at the reaction temperature of 80°C while the 60°C reaction temperature gives more isolated Ti species, also confirmed by previous DRUV results shown in Fig.5.3. Moreover, the surface area of solid catalyst prepared at 60°C is higher, thus it provides higher active sites per unit volume of catalyst and higher number of isolated Ti sites.

5.5 Conclusions

Silatrane and titanium glycolate precursors synthesized from the OOPS process was successfully used to prepare the Ti-MCM-41 catalyst. The structure of MCM-41 is not affected by the increase of Ti-loading. The BET surface area was as high as 2300 m^2/g for Ti loading in the range of 1-5%. The Ti incorporation is mainly in the form of isolated Ti species when Ti loading is not more than 10% as probed by DRUV. The hexagonal pore structure was observed using XRD and TEM. The pore sizes are very uniform as shown by the presence of sharp and clear separation of 100, 110 and 200 reflections peaks and sharp inflection of N_2 adsorption isotherm. The peroxidative bromination test showed good activity of the synthesized catalyst for both catalysts prepared at 60° and 80°C. However, the

activity of catalyst prepared at 60°C is higher due to the presence of higher concentration of isolated Ti species.

5.6 Acknowledgements

This research work is supported by the Postgraduate Education and Research Program in Petroleum and Petrochemical Technology (ADB) Fund, Ratchadapisake Sompote Fund, Chulalongkorn University and the Thailand Research Fund (TRF).

5.7 References

1. Phillip ES, Richard AC. *J. Phys. Chem. B* 1999; **103**: 1084.
2. Beck JS, Vartuli JC, Roth WJ, Leonowicz ME, Kresge CT, Schmitt KD, Chu C, Olson DH, Sheppard EW, McCullen SB, Higgins JB, Schlenker JL. *J. Am. Chem. Soc.* 1992; **114**: 10834.
3. Haskouri JE, Cabrera S, Caldes M, Alamo J, Beltran-Porter A, Marcos MD, Amoros P, Beltran-Porter D. *Int. J. Inorg. Mater.* 2001; **3**: 1157.
4. Haskouri JE, Cabrera S, Caldes M, Alamo J, Beltran-Porter A, Marcos MD, Amoros Beltran-Porter D. *Chem. Mater.* 2002; **14**: 2637.
5. Cabrera S, Haskouri JE, Carmen G, Julio L, Beltran-Porter A, Beltran-Porter D,Marcos M D, Amoros P. *Solid State Science* 2000; **2**: 405.
6. Sathupanya M, Gulari E, Wongkasemjit S, *J. Eur. Cer. Soç* 2002; **22**: 1293.
7. Sathupanya M, Gulari E, Wongkasemjit S, *J. Eur. Cer. Soc.* 2003; **23**, 2305.
8. Phiriyawirut P, MagarJaphan R, Jamieson AM, Wongkasemjit S. *Mat. Sci. Eng.* 2003; **A361**: 147.
9. Charoenpinijkarn W, Sawankruhasn M, Kesapabutr B, Wongkasemjit S, Jamieson AM. *Eur. Polym. J.* 2001; **37**: 1441.
10. Thitinum S, Thanabodeekij N, Jamieson AM, Wongkasemjit S, *J. Eur. Cer. Soc.* 2003; **23**: 417.

11. Phonthammachai N, Chairassameewong T, Gulari E, Jamieson AM, Wongkasemjit S. *J. Met. Mat. Min.* 2003; **12**: 23.
12. Marchese L, Maschmeyer T, Gionotti E, Dellarocca V, Rey F, Coluccia S, Thomas JM. *Phys. Chem. Chem. Phys.* 1999; **1**: 585.
13. Ettireddy PR, Lev D, Panagiotis GS. *J. Phys. Chem. B* 2002 ; **106** : 3394.
14. Hannus I, Toth T, Mehn D, Kiricsi I. *J .Mol. Struc.* 2001; **563-564** : 279.
15. Gianotti E, Frache A, Coluccia S, Thomas JM, Maschmeyer T, Marchese L. *J. Mol. Cat. A: Chem.* 2003; **204-205**: 483.
16. Marchese L, Maschmeyer T, Gionotti E, Coluccia S, Thomas JM. *J. Phys. Chem. B.* 1997; **101**: 8836.
17. Chatterjee M, Hayashi H, Siato N. *Micropor. Mesopor. Mater.* 2003; **57**: 143
18. Shan Z, Jansen JC, Marchese L, Maschmeyer Th. *Micropor. Mesopor. Mater.* 2001; **48**: 181.
19. Blasco T, Corma A, Navarro MT, Pariete P. *J. catal.* 1995; **156**: 65.
20. Haskouri JE, Cabrera S, Gutierrez M, Beltran-Porter A, Beltran-Porter D, Marcos MD, Amoros P. *Chem. Commun.* 2001; **7**: 1437
21. Haskouri JE, Zarate DO, Perez-Pla F, Cervilla A, Guillem C, Latorre J, Marcos MD, Beltran A, Beltran D, Amoros P. *New J. Chem.* 2002; **26**: 1093.
22. Frye C, Vicent G, Finzel W. *J. Am. Chem. Soc.* 1971; **93**: 6805.
23. Schacht S, Janicke M, Schuth F. *Micropor. Mesopor. Mater.* 199; **22**: 485.
24. Liu Z, Sakamoto Y, Ohsuna T, Hiraga K, Terasaki O, Ko CH, Shin HJ, Ryoo R. *Angew. Chem. Int. Ed.* 2000 ; **39**: 3107.
25. Maria DA, Zhaohou L, Jacek K. *J. Phys. Chem.* 1996; **100**: 2178.
26. Bharat IN, Olanrewaju J, Komarneni S. *Chem. Mater.* 2001; **13**: 552.
27. Rajakovic VN, Mintova S, Senker J, Bein T. *Mat. Sci. Eng. C* 2003 ; **23** : 817.
28. Clague MJ, Bulter A. *J. Am. Chem. Soc.* 1996; **117**: 3475.
29. Raimondi ME, Gianotti E, Marchese L, Martra G, Maschmeyer T, Seddon JM, Coluccia S. *J. Phys. Chem. B* 2000; **104**: 7102.
30. Khushalani D, Ozin GA, Kuperman A. *J. Mater.Chem.* 1999; **9**: 1483
31. Khushalani D, Ozin GA, Kuperman A. *J. Mater.Chem.* 1999; **9**: 1491.
32. Thanabodeekij, N., Gulari, E. and Wongkasemjit, S., Accepted for publication in Materials Chemistry and Physics.

33. Clague MJ, Keder NL, Bulter A. *Inorg. Chem.* 1993; **32**: 4754.

34. Sozedjak HS, Bulter A. *Inorg. Chem.* 1990; **29**: 5015.

35. Walker JV, Morey M, Carlsson H, Davidson A, Stucky DG, Bulter A. *J. Am. Chem. Soc.* 1997; **119**: 6921.

Table 5.1 The BET analysis of Ti-MCM-41 synthesized at different Ti loading Temperature

% Ti	BET Surface Area (m2/g)	Pore Volume (cc/g)	Average Pore size (nm)
60°C			
1	2351	1.21	2.07
3	2371	1.28	2.11
5	2314	1.38	2.19
15	1827	1.26	2.33
20	1834	1.19	2.58
30	1864	1.23	2.64
35	1707	1.39	2.78
80°C			
1	2324	1.41	2.33
3	2475	1.61	2.32
5	2417	1.66	2.32
15	1711	1.29	2.55
20	1705	1.26	2.66
30	1724	1.23	2.65
35	1600	1.12	2.81

Table 5.2 The EDS analysis of Ti-MCM41 synthesized at different Ti loading and temperature

Temp	**%Ti loaded**							
(°C)	**3**	**5**	**10**	**15**	**20**	**25**	**30**	**35**
60	2.96	5.06	10.38	15.6	20.62	24.57	28.68	32.87
80	2.95	5.22	10.64	15.43	20.22	24.85	28.58	33.01

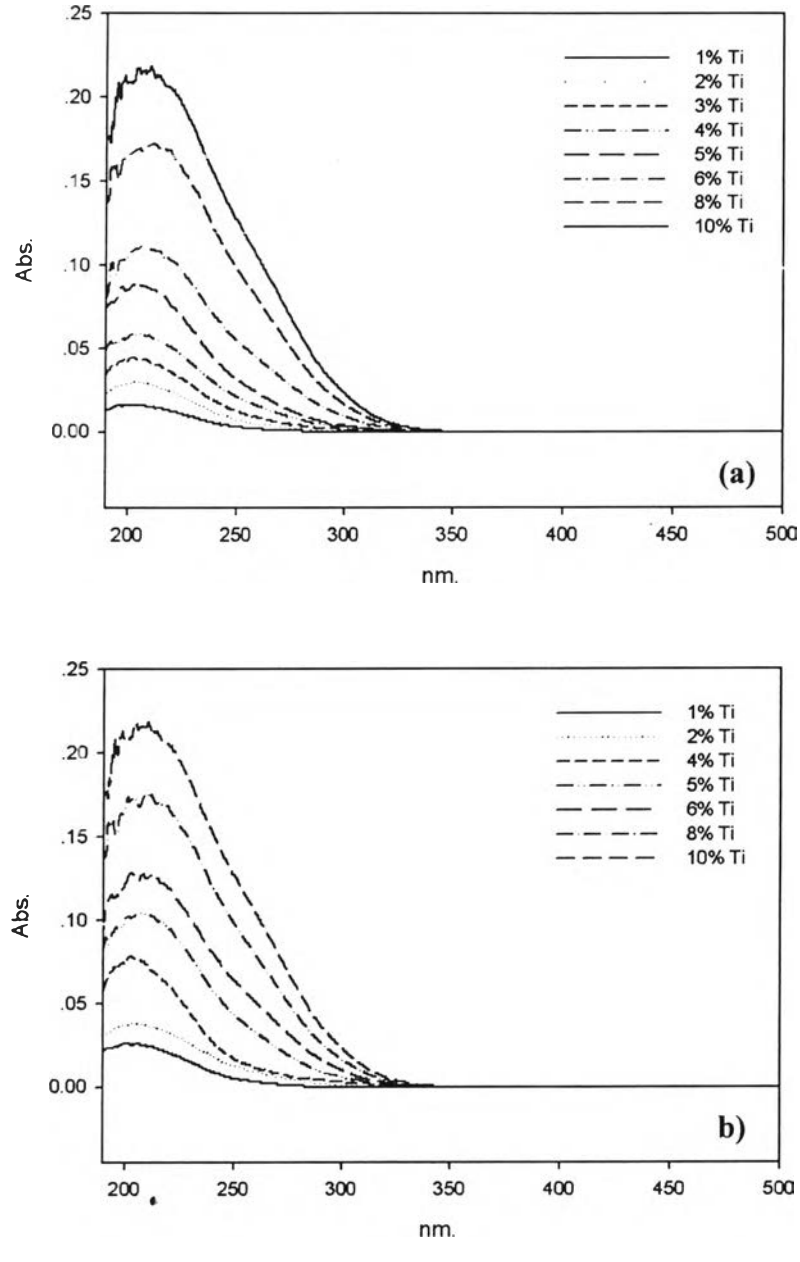

Figure 5.1 DRUV spectra of Ti-MCM-41 containing %Ti loading of 1-10% at **(a)** 60° and **(b)** 80°C.

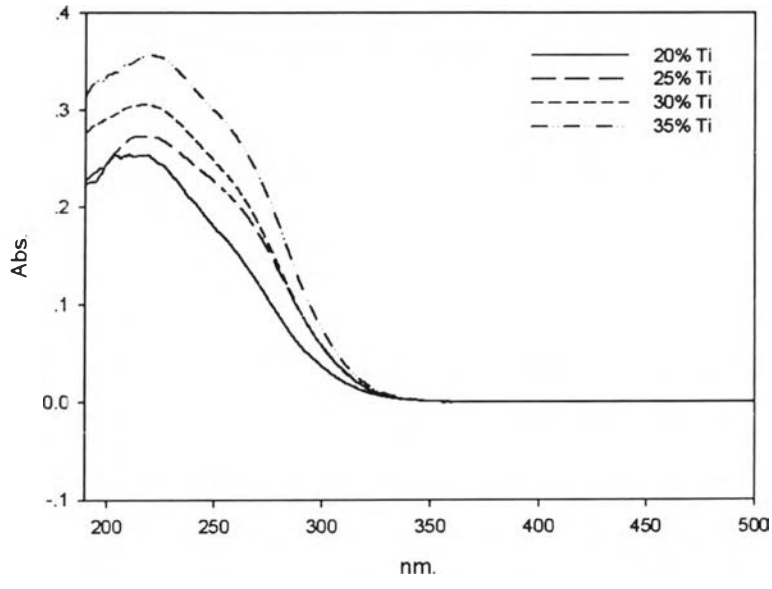

Figure 5.2 DRUV spectra of Ti-MCM-41 at various %Ti loadings.

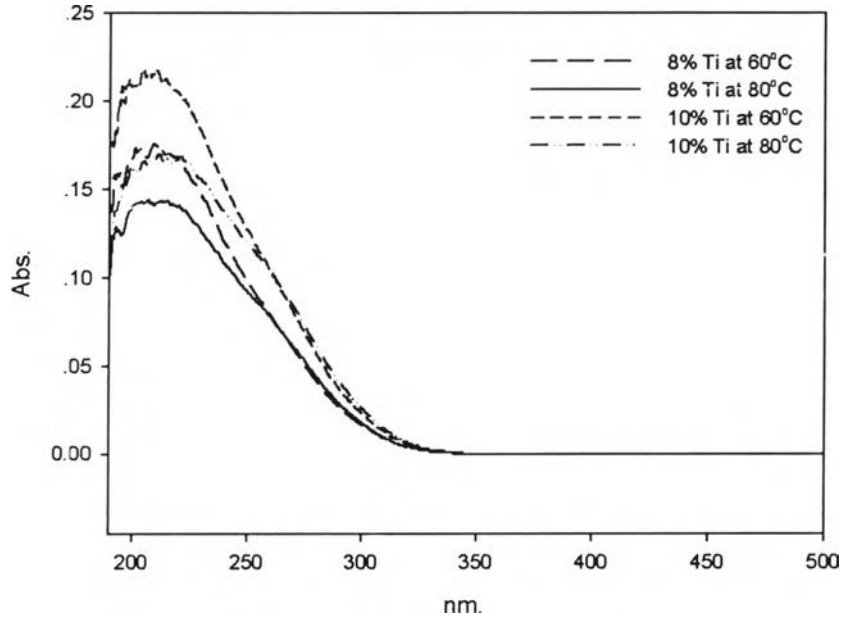

Figure 5.3 Comparison of DRUV spectra of Ti-MCM-41 at Ti loadings of 8% and 10% at the reaction temperature of 60° and 80°C.

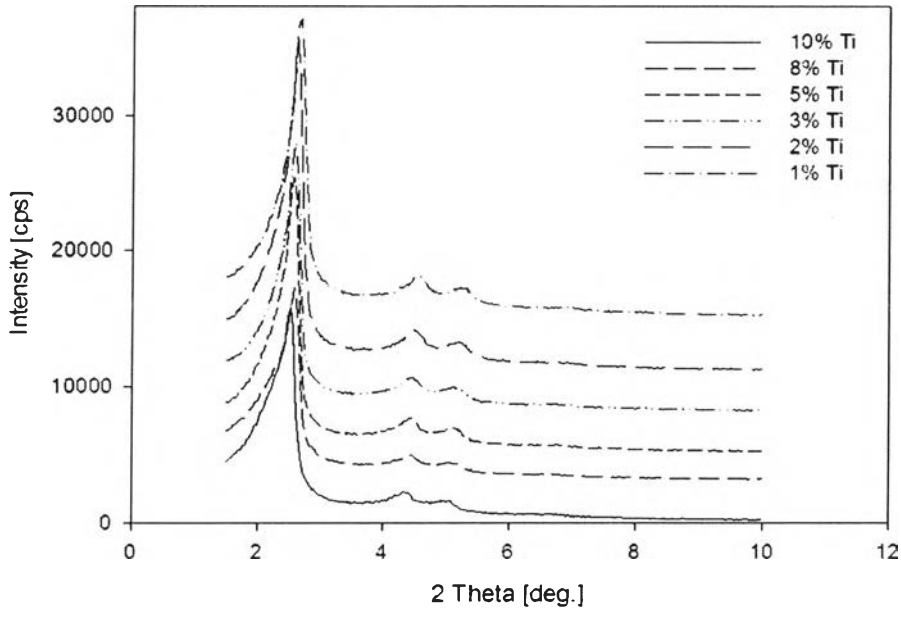

Figure 5.4 XRD spectra of Ti-MCM-41 containing various Ti loadings.

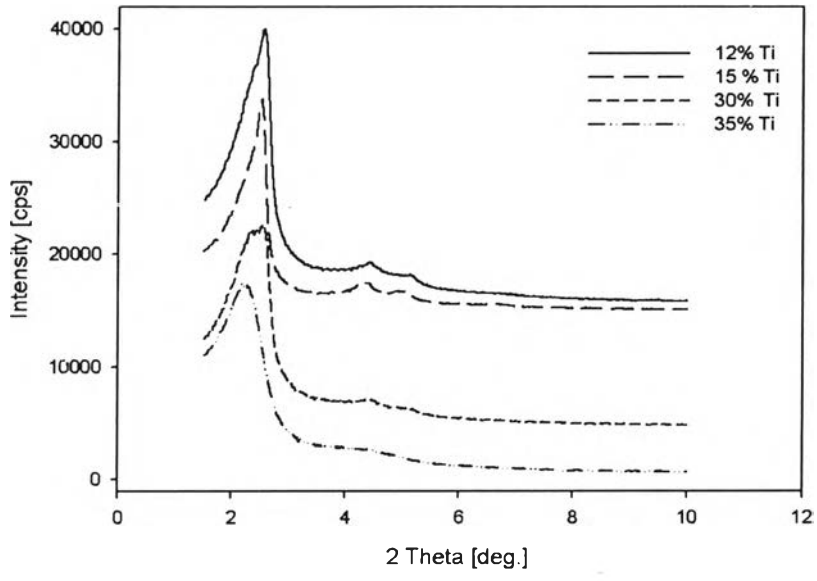

Figure 5.5 XRD spectra of Ti-MCM-41 at Ti loadings of 12, 15, 30 and 35%.

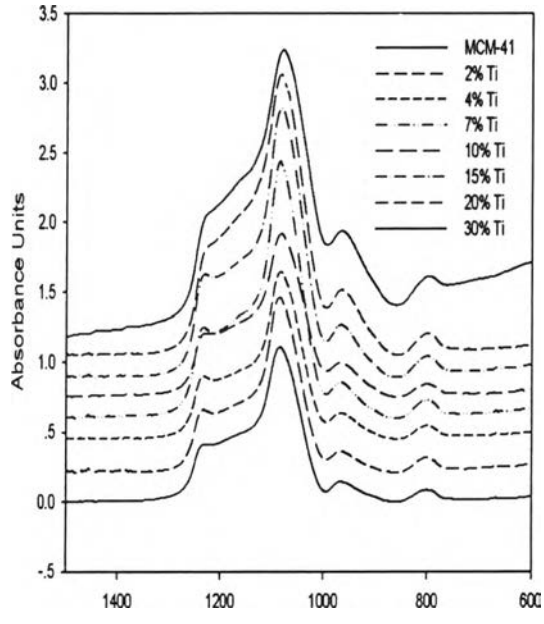

Figure 5.6 FTIR spectra of Ti-MCM-41 containing various Ti loadings.

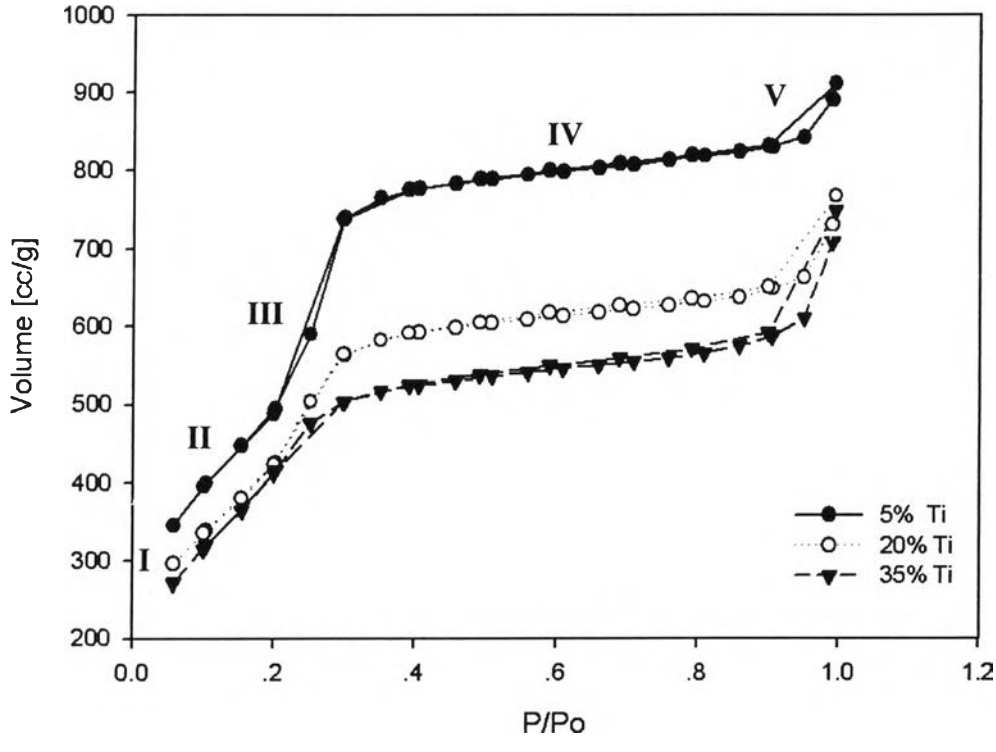

Figure 5.7 Comparison of N_2 adsorption isotherm of Ti-MCM-41 at various % Ti Loadings.

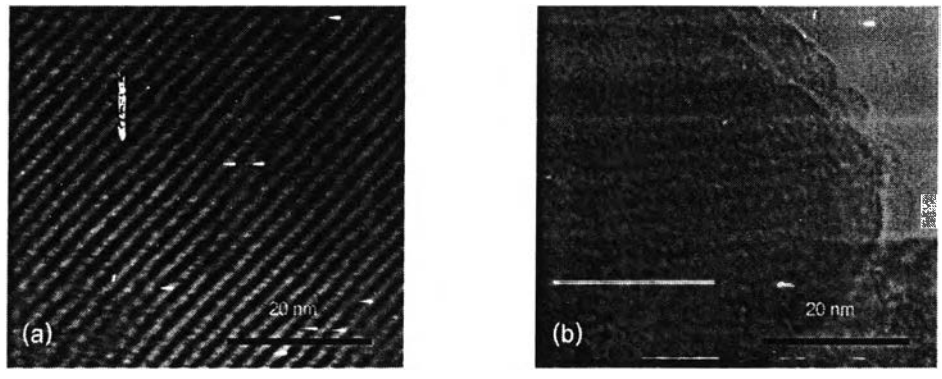

Figure 5.8 TEM images in perpendicular direction of: **(a)**. MCM-41 and **(b)**. 5% Ti loaded MCM-41obtained at the reaction temperature of 60°C.

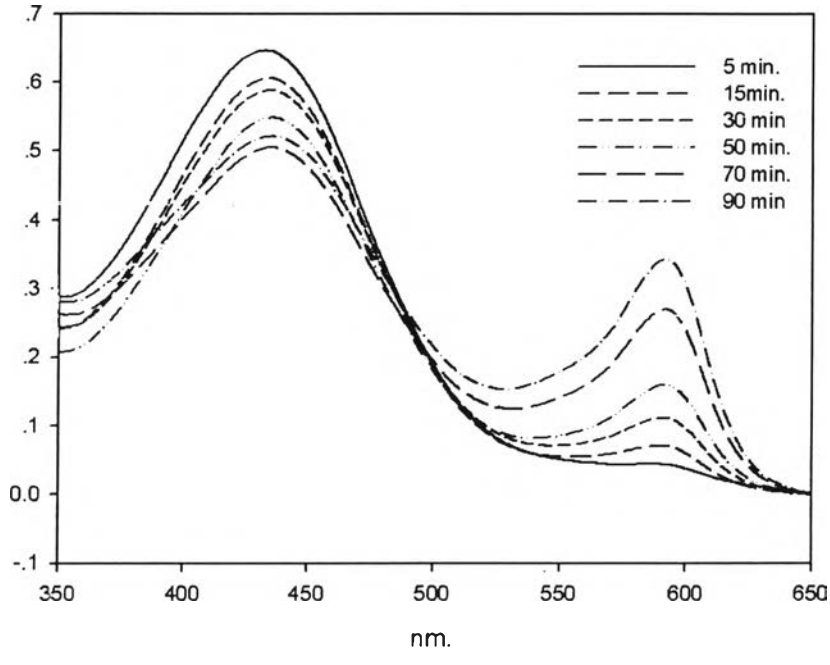

Figure 5.9 UV-vis absorption spectra of solutions peroxidatively brominated phenolsulfonephthalein (phenol red) catalyzed by Ti-MCM-41, and taken after 5, 15, 30, 50, 70 and 90 min.

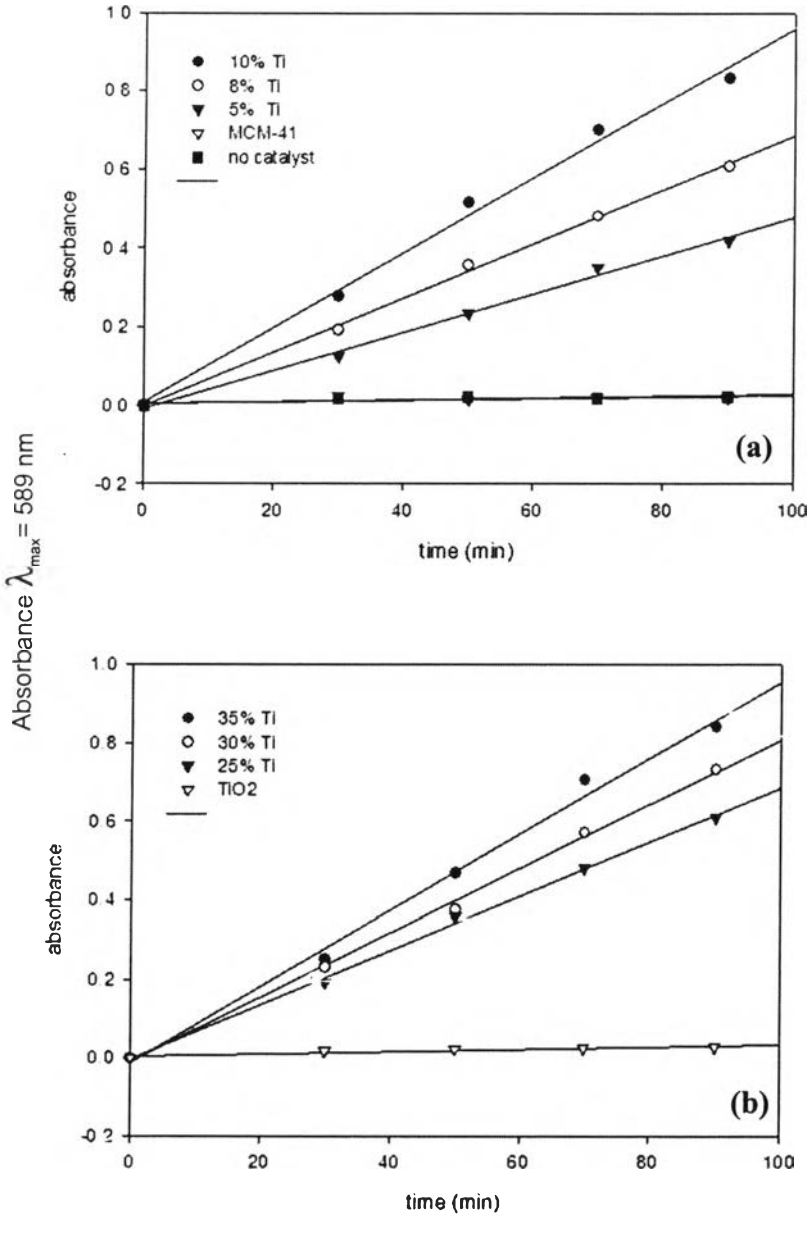

Figure 5.10 Comparison of the peroxidative bromination reaction at various % Ti loadings using: **(a)**. 5 and **(b)**. 3 mg of catalyst.

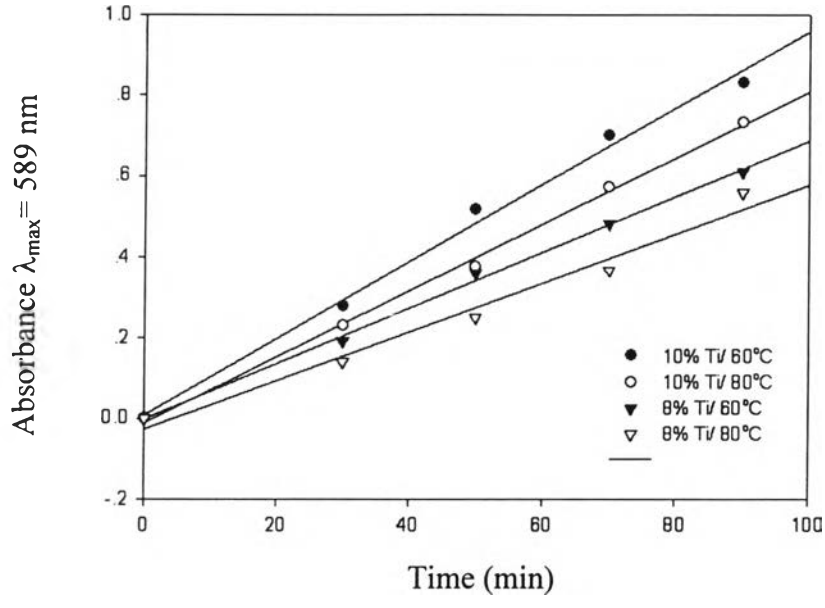

Figure 5.11 Comparison of catalyst activity of Ti-MCM-41 at Ti loading of 30 and 35% prepared at the reaction temperature of 60° and 80°C.